ISSN 1061-8309, Russian Journal of Nondestructive Testing, 2015, Vol. 51, No. 8, pp. 513–519. © Pleiades Publishing, Ltd., 2015.
Original Russian Text © A.I. Potapov, V.A. Syas'ko, O.P. Pudovkin, 2015, published in Defektoskopiya, 2015, Vol. 51, No. 8, pp. 64–71.

Optimization of the Parameters of Primary Measuring Transducers that Use the MFL Technology

A. I. Potapov[a], V. A. Syas'ko[b], and O. P. Pudovkin[c]

[a]*Northwestern State Correspondence Technical University, ul. Millionnaya 5, St. Petersburg, 191186 Russia*
e-mail: apot@mail.ru
[b]*OOO Konstanta, ul. Marshala Govorova 29, St. Petersburg, 198097 Russia*
e-mail: 9334343@rambler.ru, office@constanta.ru
[c] *National Mineral Resource University (University of Mines), 21 liniya 2, St. Petersburg, 199106 Russia*
e-mail: pudovkin.oleg@gmail.ru

Received January 29, 2015

Abstract—The problems of optimizing the magnetic system of primary measuring transducers that use the magnetic-flux leakage technology using the finite-element method are considered. The main calculation results and the development of transducers for testing pitting–corrosion flaws of petrochemical objects are presented.

Keywords: magnetic-flux leakage, leakage magnetic field, corrosion, pitting–corrosion flaws, magnetic testing, finite-element modeling

DOI: 10.1134/S1061830915080070

The magnetic-flux leakage (MFL) technology (a magnetic technology for nondestructive testing (NDT) that uses the Hall-effect method for analyzing the leakage magnetic field of a flaw in accordance with GOST (State Standard) 24450–80) is widely used by such leading companies as Silverwing, Rosen, NDT Technologies, Intron plus, and Spetsneftegaz, which produce the equipment for detecting:

corrosion flaws (pitting or planar) of walls of items that are produced of ferrous metals, mainly pipelines and bottoms of cylindrical reservoirs (e.g., oil reservoirs);

mechanical damage (longitudinal and transverse ruptures or cracks with large openings) of seamless and welded pipes, including thick-wall pipes; and

defects of longitudinal weld seams in pipes.

Let us consider the main concepts of this method. When a U-shaped permanent magnet is positioned at a certain distance from the wall of a ferromagnetic object, some of the lines of force are interrupted at the interface between two media (magnet–air and air–object wall) with different values of the absolute permeability μ_i, and the normal H_{ni} component of the magnetic-field strength H undergoes a jump:

$$\begin{cases} \operatorname{div} B = \operatorname{div} \mu H, \\ \operatorname{div} B = \mu_1 H_{n1} - \mu_2 H_{n2} = 0. \end{cases} \quad (1)$$

Hence, it follows that $\mu_1 H_{n1} = \mu_2 H_{n2}$ and the magnetic lines of force are refracted according to the tangent law [1]. When rare-earth magnets (Nd–Fe–B) with the induction $B_m \sim 1$–1.12 T are used, the magnetic lines of force at the air–steel interface are directed almost perpendicular to the surface, while in the object volume, they tend to pass almost in parallel to the surface, thus providing a minimum reluctance of the magnetic circuit. At certain relationships between the thickness, T, of the object wall (sheet) and the dimensions of the magnet, almost all magnetic-flux (MF) lines of force run inside the sheet and only an insignificant part of them will be outside (Fig. 1a).

If an area with local thinning (e.g., owing to pitting corrosion) occurs on one of the sheet surfaces, the magnetic-field pattern will be modified (Fig. 1b). The density of the lines of force near a flaw will increase and a part of the magnetic lines of force will leave the sheet from the side where the magnet is installed and from the opposite side (MF scattering will occur). This can be determined by measuring the normal

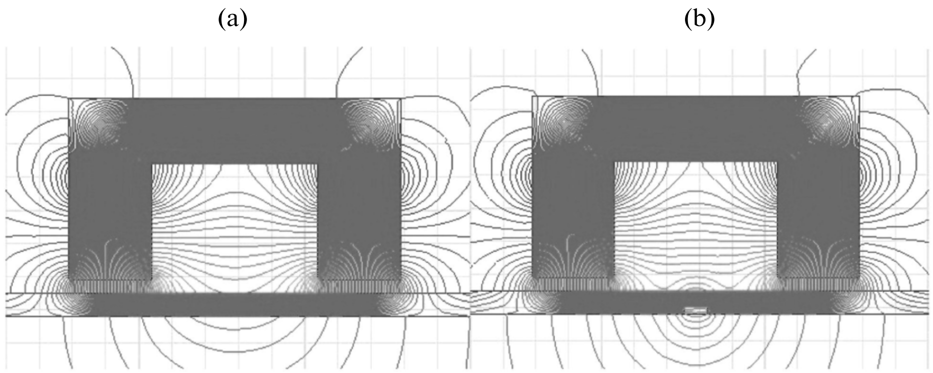

Fig. 1. The calculated pattern of (a) the magnetic-field lines of force on a defect-free area of a steel sheet and (b) the leakage magnetic-field lines in the region of an artificial flaw.

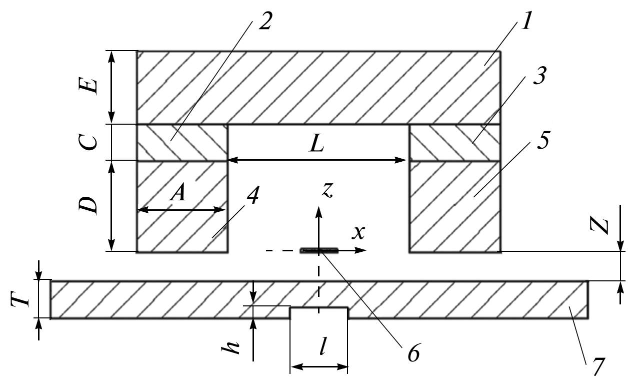

Fig. 2. A primary measuring transducer that uses the MFL technology and a test object with an artificial flaw in the form of a transverse kerf that simulates a corrosion damage of the wall: (*1*) magnetic-circuit yoke, (*2*, *3*) rare-earth magnets, (*4*, *5*) poles of the magnetic circuit, (*6*) sensitive element/observation point; and (*7*) steel sheet with an artificial flaw.

H_n component of the magnetic-field strength or the MF Φ_i that penetrates through a solid-state sensitive element with the area S, which is parallel to the sheet surface:

$$\Phi_i - \oint_s B_n dS - \oint_s \mu_{\upsilon} H_n dS, \tag{2}$$

where B_n and H_n are, respectively, the normal components of the magnetic induction and magnetic-field strength at the measurement point, which is positioned symmetrically between the magnet poles.

Primary measuring transducers (hereinafter, transducers) that use the considered NDT technology are U-shaped magnetic circuits with inserts of permanent rare-earth magnets (Nd–Fe–B) and a multichannel system of sensitive elements that are positioned symmetrically between the magnetic-circuit poles in the region of a magnetic field of the same intensity (Fig. 2). The basic transducers of the Silverwing Company, which is one of the founders of this technology, have the following dimensions: the magnet length is $A = 25$ mm; the magnet height is $C = 10$ mm, the yoke height is $E = 20$ mm; the pole height is $D = 25$ mm; the distance between the poles is $L = 50$ mm; and the technological gap is $Z = 5$ mm. The width of the magnetic circuit is 40 mm. The transducers are intended for detecting the planar and pitting corrosion of items with wall thicknesses T of 6–16 mm. At $l \approx T$, it is assured that artificial flaws with depths (h) of 1.8 ($T = 6$ mm) to 8 mm ($T = 16$ mm) will be detected. As sensitive elements, Hall probes are used that analyze changes in the component B_z of the magnetic induction at the observation point upon a displacement of the transducer relative to a flaw along the x axis (the origin of the coordinate system is locked to the kerf center).

It was shown in [2] that the efficient use of the MFL technology for particular objects requires one to design an optimal measuring system that corresponds to a particular problem, as well as the application of special methods for processing measurement information and an adequate interpretation of the results.

The transducer sensitivity, which is characterized by a change in the amplitude $B_z(h)$ in the corrosion-damage zone, will probably not be optimal for all points in the ranges of T and h changes.

The main parameters of the quality of a transducer are as follows:

the transducer sensitivity $dB_z(h, T)/dh$, which determines the measurement error $\Delta h(h, T)$ and the measurement range $h_{\min}$–$h_{\max}$;

the minimum possible dimensions of the magnetic circuit that provide the predetermined $\Delta h(h, T)$ and $h_{\min}$–$h_{\max}$ in the required thickness range $T_{\min} - T_{\max}$;

the mass–dimensional and ergonomic characteristics.

To provide the required quality indices, a compromise solution must be sought, as these indices are interrelated.

When analyzing a transducer (Fig. 2), we assume that the magnetic-circuit width is much larger than its height, C, and length, A, thus allowing the influence of the width to be excluded from the calculations.

The finite-element method (FEM) is widely used to solve problems that are related to the analysis of electromagnetic fields [3].

The desired values of the parameters will be calculated at node points (nodes), which are common points of finite elements. The scalar magnetic potential, φ^{M}, of each finite element is represented in the form of a polynomial with coefficients that are constant within this element:

$$\varphi^{\mathrm{M}} = a_i + b_i x + c_i y. \tag{3}$$

The main task of the calculation using the FEM is to determine the a_i, b_i, and c_i coefficients. After these coefficients are found it becomes possible to calculate the magnetic potential at any spatial point of the model. The initial data, which are complemented by the boundary conditions, and the energy dependences lead to a system of algebraic equations, which allows the calculation of the desired coefficients of the polynomials in all finite elements [4].

As applied to the considered problem for the boundary conditions of the first kind (Dirichlet conditions), the minimized functional is the quantity that is proportional to the stored spatial magnetic energy:

$$W_{\mathrm{M}} = 0.5\int \mu\mu_0 H^2 dv. \tag{4}$$

Since $H = -\mathrm{grad}\,\varphi^{\mathrm{M}}$, the minimized functional can then be written in the form

$$W_{\mathrm{M}} = 0.5\int \mu\mu_0 (\mathrm{grad}\,\varphi^{\mathrm{M}})^2 dv, \tag{5}$$

and the desired (minimizing) function is $\varphi^{\mathrm{M}}(\xi, \zeta, \eta)$, at which $W_{\mathrm{M}}\{\varphi^{\mathrm{M}}\} \geq \min$. The sum of the magnetic energies that are stored in all finite elements serves as the functional. In this model, the elements touch one another at common (node) points. The energy of the elements is determined by the magnetic potentials of the node points $W = W\{\varphi_1, \varphi_2, \ldots, \varphi_N\}$, where N is the number of points.

On the basis of the analysis and determination of the magnetic potentials of the common (node) points at which W_{M} reaches a minimum, a system of algebraic equations is formed, the magnetic potentials are calculated, and the magnetic induction and magnetic-field strength are calculated [5].

The optimal geometric characteristics of a transducer are considered to mean such characteristics and their relationships at which the maximum sensitivity is attained within the required region, $h_{\min}$–$h_{\max}$, of measured test objects within the $T_{\min}$–$T_{\max}$ wall-thickness range at the minimum possible dimensions.

When software products are used that use the FEM, the following statement of the transducer calculation problem can be formulated: a 2D, axially symmetric, stationary, generally nonlinear problem with open boundaries and the following assumptions: in a sufficiently remote zone from the transducer, the magnetic field that it produces is infinitesimal; external magnetic fields are absent; and the model is fully stationary (no time and temperature drifts of the transducer's physical characteristics occur).

According to the first two assumptions, the boundary conditions of the first kind can be taken as the boundary conditions for models of the considered transducers. This boundary condition is applicable for specifying the zero value of the normal component of the magnetic-induction vector on the axis of symmetry (at the observation point) and indicating the complete field damping at boundaries that are conditionally infinitely far from the transducer. The variable parameters are the sheet thickness, T, the relative

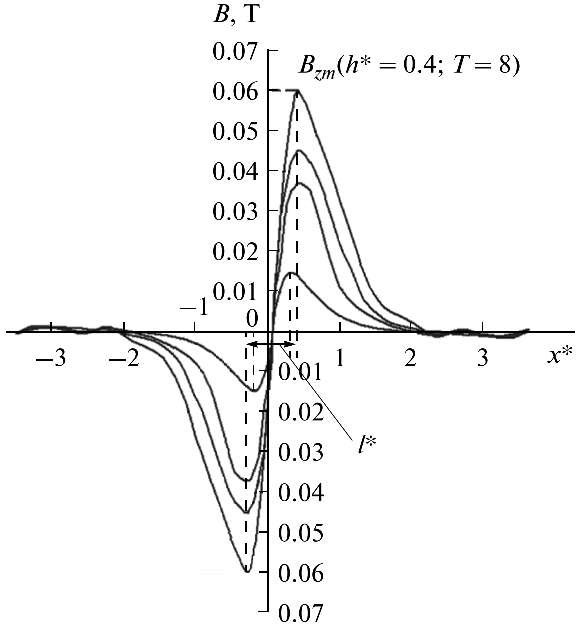

Fig. 3. The dependence $B_z(h^*, x^*)$ above a 1010 steel sheet with a thickness of $T = 8$ mm in the vicinity of a transverse kerf with a width of $l^* = 1$ at $Z = 5$ mm.

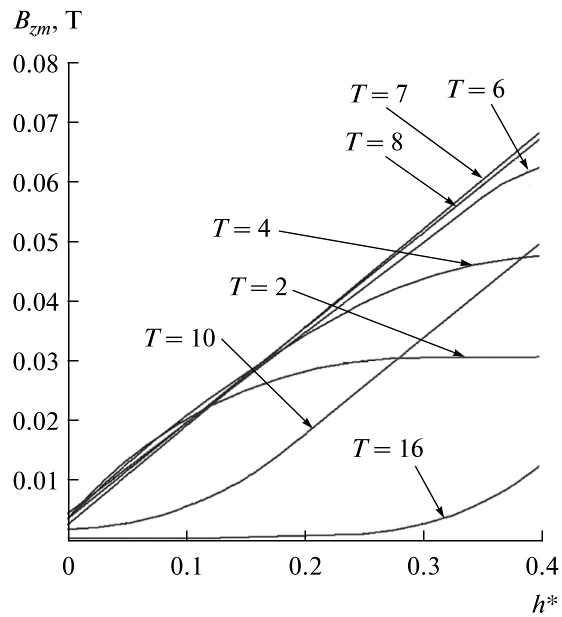

Fig. 4. The dependence $B_{zm}(h^*, T)$ above a 1010 steel sheet with an artificial flaw in the form of a transverse kerf with a width of $l^* = 1$ at $Z = 5$ mm.

coordinate $x^* = x/T$, and the relative depth $h^* = h/T$ at a constant relative width of the kerf $l^* = l/T = 1$. In the calculations, the structural gap and the magnetic induction in the magnetic circuit are assumed to be $Z = 5$ mm and $B_m \approx 1.12$ T, respectively.

As an example, Fig. 3 shows the calculated dependences $B_z(h^*, x^*)$ at a symmetric position of the transducer (relative to the kerf) for $Z = 5$ mm and $T = 8$ mm, which show that the maximum value of $B_{zm}(h^*)$ is reached at the edges of the kerf at $|x^*| \approx 0.5$, and near the middle of the kerf, $B_z(h^*, x^* = 0) \approx 0$.

Figure 4 shows the calculated dependences $B_{zm}(h^*, T)$ for the considered transducer model above a ferromagnetic sheet of 1010 steel (an analog of Ст10) with an artificial flaw in the form of a transverse kerf, which is made in accordance with Fig. 2.

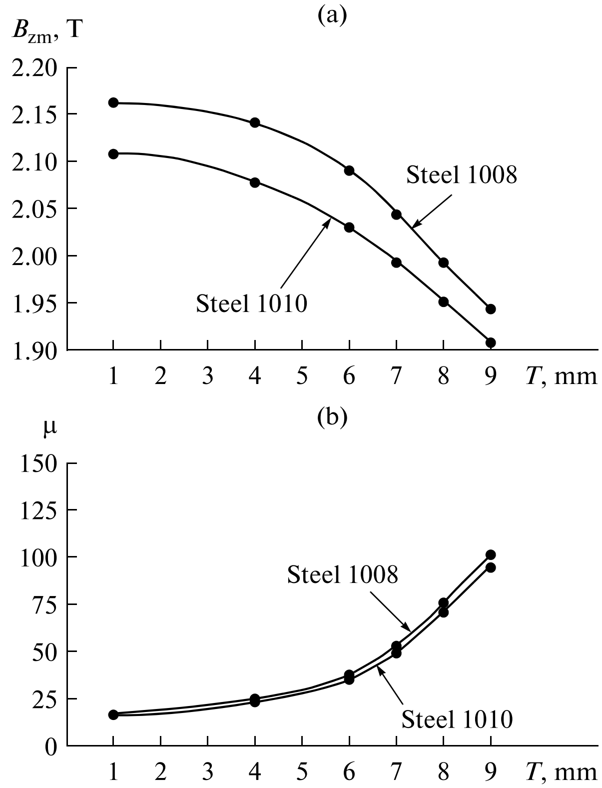

Fig. 5. The dependences of (a) the magnetic induction, B_m, and (b) the relative magnetic permeability, μ, in a metal sheet on its thickness, T, in the zone of mounting the sensitive element.

As is seen, in the range $h^* \approx 0.05–0.4$, the transducer has the highest sensitivity at $T \approx 6–8$ mm. If $T <$ 4 mm; significant nonlinearity of the characteristic and a decrease in the sensitivity are observed at $h^* >$ 0.1–0.2. At $T > 10$, the transducer becomes almost completely insensitive at $h^* < 0.15$. Calculations show that for $h^* \approx 0.05–0.35$, similar characteristics occur in a range of $T \approx 5–9$ mm. Hence, a conclusion can be drawn about the value of the optimal metal magnetization for performing testing.

Figure 5 shows the calculated values of the magnetic induction, $B_m(T)$, and the relative magnetic permeability, $\mu(T)$, of a metal sheet, which is magnetized with the transducer (depending on T) for 1010 and 1008 steels (the characteristics of the latter are similar to those of Ст0) in the zone where the sensitive element is installed at $h^* = 0$. In accordance with the above, the optimal value is $1.9 < B_m < 2.05$ T. To perform testing, a metal should be magnetized to a value that corresponds to $30 < \mu < 70$.

Let us introduce the relative dimensions of the transducer: $A^* = A/T$; $C^* = C/T$; $E^* = E/T$; $D^* = D/T$; $L^* = L/T$; and $Z^* = Z/T$. For $T_0 = 7$ mm, the values $A_0^* = 3.57$; $C_0^* = 1.43$; $E_0^* = 2.86$; $D_0^* = 3.57$; $L_0^* = 7.14$; and $Z_0^* = 0.71$ are denoted as the optimal values for the considered transducer. In a testing range of $\Delta T = 5–9$ mm, the relative dimensions of the transducer will change within the following ranges: $\Delta A^* \sim (5–2.77)$; $\Delta C^* \sim (2–1.11)$; $\Delta E^* \sim (4–2.22)$; $\Delta D^* \sim (5–2.77)$; $\Delta L^* \sim (10–5.55)$; and $\Delta Z^* \sim (1–0.55)$.

In accordance with Fig. 2 (provided that the magnetic systems of transducers are similar), the entire range of tested thicknesses, T, can be divided into subranges, for each of which the relative dimensions of transducers correspond to the optimal ones and change within the limits that are preset for them. The table presents the calculated dimensions of the magnetic system of transducers and the measurement ranges that correspond to the formulated requirements.

When detecting the locations of pitting–corrosion flaws of large tested objects, for example, oil tanks or trunk pipelines, one of the main interfering parameters is the local deviation Δμ of the relative permeability, which may reduce the reliability of the testing results [6]. To perform estimates, we calculated $B_{zm}(h^*, T)$ for 1010 and 1008 steels (Fig. 6); the difference of their magnetic properties is comparable to the possible local deviation Δμ for these test objects. In this case, during surface scanning, the deviation is

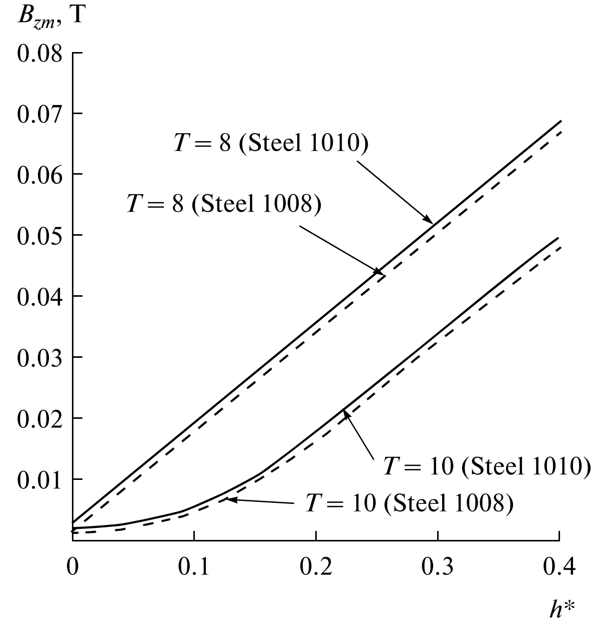

Fig. 6. The dependence, $B_{zm}(h^*, T)$, above a ferromagnetic sheet of 1010 and 1008 steels with an artificial flaw in the form of a transverse kerf with a width of $l^* = 1$ at $Z = 5$ mm.

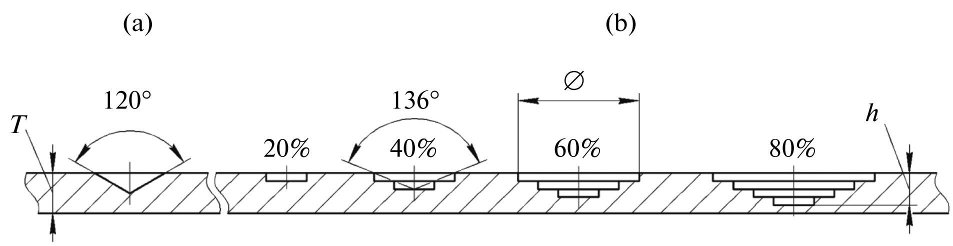

Fig. 7. Reference specimens with artificial flaws: (a) conical flaw with a depth of $0.4T$ and (b) stepped conical flaws with depths of $0.2–0.8T$ that simulate pitting–corrosion flaws.

$B_{zm}(h^*, T) = |B_{zm}(h^*, T)_{1010st} - B_{zm}(h^*, T)_{1008st}| < 0.002$ T in virtually the entire range of h^*. This will not lead to an appreciable decrease in the measurement error of the depth and dimensions of pitting–corrosion flaws.

The gap Z deviation (for example, a protective-coating thickness) will also lead to a change in the transducer sensitivity and an uncertainty in the evaluation of the pitting–corrosion depth, because $B_{zm} \sim 1/Z$, other conditions being equal [7].

Until recently, reference specimens that were used in the petrochemical industry for calibrating measuring transducers that use the MFL technology were metal sheets whose thickness and composition were identical to those of actual products and that had conical drilled holes with an angle of 120° and depths of $0.2–0.8T$ (Fig. 7a). These specimens made it possible to adjust equipment and detect pitting–corrosion flaws with high reliability. However, experiments that have been performed by leading manufacturers demonstrate that a more promising technique is the use of reference specimens with conically shaped stepped

The calculated values of the dimensions of the magnetic system of transducers and the ranges of tested thicknesses

N	T_0, mm	A, mm	C, mm	E, mm	D, mm	L, mm	Z, mm	ΔT, mm
1	3.8	13.6	5.4	10.8	13.6	27.2	2.7	2.7–5.3
2	7	25	10	20	25	50	5	5–9
3	12	42.8	17.1	34.3	42.8	85	8.5	9.2–15.9

artificial flaws with an angle of 136° and depths h of $0.2–0.8T$ (Fig. 7b), which were manufactured using gate cutters. In this case, the diameter of an artificial flaw is $\varnothing = T$ for $h^* = 0.2$ and $\varnothing = 2T$ for $h^* = 0.4$.

The use of the latter generation of small integral Hall probes (e.g., A1395 by Allegro) with a mounting step of ~1 mm makes it possible to reveal corrosion flaws with a depth of $h^* = 0.15$ for test objects with wall thicknesses of $T_{\min} \geq 2.7$ mm.

Prototype measuring transducers showed the convergence of the modeling and calculation results to the experimental data, in particular, a decrease in $\Delta h(h, T)$ upon extension of the h^* and T ranges. Tuning the transducers using reference specimens before the beginning of their operation makes it possible to inspect objects with wall thicknesses, T, of 2.7– 16 mm and measure the depth, h^*, of pitting–corrosion flaws in a range of 0.15–0.4 with an absolute tolerable error $\Delta h \leq 0.1h$, which is comparable to the error in ultrasonic thickness gauging [8].

REFERENCES

1. *Nerazrushayushchii kontrol'. Spravochnik v 7 t. pod obshch. red. V.V. Klyueva. T. 6., kn. 1. Magnitnye metody kontrolya* (Nondestructive testing. Handbook in 7 vols. Book 1, Magnetic Testing Methods), Klyuev, V.V., Ed., Moscow: Mashinostroenie, 2004, vol. 7, p. 375.
2. Slesarev, D.A. and Abakumov, A.A., Data processing and representation in the MFL method for nondestructive testing, *Russ. J. Nondestr. Test.*, 2013, vol. 49, no. 9, pp. 493–498.
3. Vishnyakov, S.V., Gordyukhina, N.M., and Fedorova, E.M., *Raschet elektromagnitnykh polei s pomosh'yu programmnogo kompleksa ANSYS* (Calculation of Electromagnetic Fields using the ANSYS Sowtware Complex), Moscow: MEI (TU), Chair of Electrophysics, 2003.
4. Andreeva, E.G., Shamets, S.P., and Kolmogorov, D.V., http://www.ogbus.ru/authors/Andreeva/Andreeva_1.pdf], *Neftegaz. Delo*, Omsk: Omsk. Gosud. Tekhn. Univer., 2005.
5. Potapov, A.I. and Syas'ko, V.A., *Nerazrushayushchie metody i sredstva kontrolya tolshchiny pokrytii i izdelii. Nauchnoe, metodicheskoe, spravochnoe posobie* (Nondestructive Methods and Facilities for Testing Thicknesses of Coatings and Items. Scientific, Methodological, and Reference Manual), St. Petersburg: Gumanistika, 2009.
6. Stanley, R., *Basic Principles of Magnetic Leakage Inspection Systems for the Evaluation of oil Country Tubular Goods. Electromagnetic Methods of Nondestructive Testing*, New York: Gordon and Breach, 1985, pp. 97–150.
7. Stenley, R., *Magnetic Leakage Field Measurements, 3 ed, vol. 8. Magnetic Testing*, Columbus: American Society for Nondestructive Testing, 2008, pp. 139–156.
8. *ASTM E 570-97. Standard Practice for Flux Leakage Examination of Ferromagnetic Steel Tubular Products.*

Translated by A. Seferov